

# How Is Starlink Manoeuvring? An Analysis of Patterns in the Manoeuvres of Starlink Satellites

David P. Shorten<sup>1</sup>, Wathsala Karunaratne<sup>1,2</sup> and Matthew Roughan<sup>1,2</sup>

<sup>1</sup>*Department of Computer and Mathematical Sciences, The University of Adelaide, Australia*

<sup>2</sup>*Teletraffic Research Centre, The University of Adelaide, Australia*

**Keywords:** Starlink, Two-Line-Element, Satellite, Manoeuvre, Space Debris, Space Situational Awareness, Particle Filter.

**Abstract:** The rapid increase in the number of active satellites orbiting earth along with the simultaneous increase in the amount of space debris is causing earth's exosphere to become ever more crowded. This crowding forces satellites to perform a rising number of collision-avoidance manoeuvres. At the time of publication, of the roughly 7700 active satellites orbiting earth, over 5000 belonged to the Starlink constellation. These satellites not only substantially contribute to the crowding of space, but are required to perform tens of thousands of collision-avoidance manoeuvres per year. As Starlink does not publish information on the timing of these manoeuvres, little is known about them beyond their total number. This work uses a recently-proposed algorithm for detecting satellite manoeuvres from the publicly-available 18<sup>th</sup> Space Defence Squadron TLE data to study the patterns in the manoeuvres of this constellation. Rich structure was found in the patterns of these manoeuvres, including regular synchronous bursts of station-keeping manoeuvres within launch groups (the groups of satellites launched on a single day) and a cyclical pattern of station keeping among the launch groups.

## 1 INTRODUCTION

Starlink is a constellation of over 5,000 satellites that provides high-speed internet access to users with an appropriate antenna (Michel et al., 2022). It has the unique advantage of being able to provide this service to users at sea or in remote regions.

The number of satellites orbiting the earth is increasing at a rapid rate. As of 1 January 2023, the list of satellites maintained by the Union of Concerned Scientists (Union of Concerned Scientists, 2023b), contained 6,718 operational satellites, an increase of nearly 2,000 satellites over the previous year (Union of Concerned Scientists, 2023a). This rate of increase is likely to accelerate. Starlink alone, which currently operates over 5000 satellites, has filed for permission to launch an additional 30,000 satellites with the Federal Communication Commission (FCC) (Boley and Byers, 2021). Other companies, including Amazon, OneWeb, Telesat and GW have announced similar plans (Boley and Byers, 2021). A total of over 100,000 satellites in orbit by 2030 is considered plausible (Venkatesan et al., 2020). This situation is further exacerbated by the large amount of space debris in orbit, which includes over 22,000 tracked ob-

jects (Pelton, 2015). The crowding of space increases the need for satellite operators to be aware of space traffic and take evasive manoeuvres when collisions are predicted. Techniques for monitoring the orbits and activities of satellites fall under the field of Space Situational Awareness (SSA) (Lal et al., 2018).

SpaceX (the operators of Starlink) are already required to perform a large number of evasive manoeuvres. According to filings with the FCC (Goldman, 2023), between the 1<sup>st</sup> of December 2022 and the 31<sup>st</sup> of May 2023, Starlink satellites performed 25,299 propulsive manoeuvres. This equates to an average of around 12 manoeuvres per satellite per year. Given that the Starlink constellation currently forms the majority of satellites in orbit, an analysis of the patterns of these manoeuvres will provide insight into the future of space traffic management.

Although Starlink is comparatively generous in their sharing of data (Goldman, 2023), they do not publish the timestamps of satellite manoeuvres. However, the 18<sup>th</sup> Space Defence Squadron provides daily updates on the orbits of all starlink satellites via Space-Track (Space-Track, 2023). This paper utilises a recently-proposed algorithm (Shorten et al., 2023a) for satellite orbit anomaly detection from this public

data in order to infer the timestamps of these manoeuvres. This approach has been thoroughly validated on a benchmark dataset (Shorten et al., 2023b) containing ground-truth manoeuvre timestamps.

We apply this anomaly detection algorithm to the historic publicly-available data of all Starlink satellites active on the 27<sup>th</sup> of November 2023. We find that the pattern of manoeuvres within the Starlink constellation exhibits rich structure. Section 3.2 explores some of the global properties of this structure, including the high rate of manoeuvres of satellites post launch. The pattern of manoeuvres across the constellation is strongly associated with the constellation’s structure. The Starlink constellation is formed of seven orbital shells, where all satellites within each shell share a common orbital altitude and inclination (see table 3 for a list). These shells can be further divided into their launch groups, consisting of the satellites launched on a single day. Section 3.3 examines the manoeuvres of a representative launch group, finding regularly-spaced stereotyped bursts of station-keeping manoeuvring where all the satellites within the launch group manoeuvre near-simultaneously. Moreover, the relative order of manoeuvring within these groups is mostly maintained over time. Section 3.4 subsequently shows how these patterns degrade over time in older satellites. This analysis is extended to the relationship in station-keeping manoeuvring between launch groups in section 3.5, where it is shown that SpaceX performs station-keeping manoeuvres on the satellites in a shell in a cyclical fashion, iteratively moving through its launch groups. Finally, section 3.6 presents an analysis of the rate of collision-avoidance manoeuvres across the constellation.

## 2 METHODS

A list of the SATCAT numbers (Kelso, 1998) of the 5044 Starlink satellites active on the 27<sup>th</sup> of November 2023 was obtained from N2YO (N2YO, 2023). The TLE data for all of these satellites was then downloaded from Space-Track (Space-Track, 2023). table 1 contains a summary of the data used in this work. TLE data consists of the mean Keplerian orbital elements of satellites, along with metadata such as a ballistic drag coefficient, recorded roughly daily (Vallado and Cefola, 2012). The timestamp associated with each record is usually referred to as the *epoch*. The orbital elements are ‘mean’ in the sense that they exclude high-frequency non-Keplerian components. That is, they specify the elliptical orbit which most closely approximates the true (non-elliptical) orbit of

Table 1: Summary statistics of Starlink satellite data.

Feature	Value
Number of Starlink satellites analysed	4,998
Total number of TLE data points	7,363,925
Total number of detected manoeuvres	129,860
Median number of manoeuvres per satellite	17
First launch date included	11/11/2019
Last launch date included	29/10/2023

Table 2: Parameters for optimal proposal filter. See (Shorten et al., 2023a) for an explanation of each parameter.

Parameter	Description	Value
$N$	Number of particles	250
$\alpha$	Variance inflation factor	3
$\tau_r$	Threshold on $N_{\text{effective}}$ for regularisation	0.2
$\tau_{\text{shift}}$	Threshold on negative log predictive density for ensemble shift	20
$\tau_{\text{anom}}$	Threshold on negative log predictive density for anomaly detection	100

the satellite.

The 46 satellites from the two most recent launches (on the 22<sup>nd</sup> and 27<sup>th</sup> of November 2023 (SpaceX, 2023)) were discarded as there was insufficient data for the operation of the anomaly detection algorithm.

A recently-proposed (Shorten et al., 2023a) satellite orbit anomaly detection algorithm was then applied to the TLE data of the remaining 4998 satellites. This approach operates by applying an optimal-proposal particle filter (Snyder, 2011) to the mean Keplerian orbital elements present in the TLE data. The idea of filtering, in this context, is to assume that the mean elements present in each TLE line pair are noisy

measurements of the true underlying values of these elements. Filtering then seeks to infer the true values of these elements at each epoch, along with an uncertainty. Particle filters are well-suited to the non-linear nature of satellite orbit evolution and allow us to compute a non-Gaussian uncertainty. The filtering setup makes use of the SGP4 (Vallado et al., 2006) model for orbit evolution. However, it only makes use of the initial part of this model which propagates the mean Keplerian elements before incorporating the high-frequency non-Keplerian components. Moreover, a non-standard implementation of SGP4 is used. Standard implementations first convert the mean motion from the Kozai to the Brouwer formulations before propagation (Vallado et al., 2006). Instead, we perform this as an initial pre-processing step, and perform no such conversions during propagation.

Once the filter has arrived at an estimate (with uncertainty) for the mean elements at a given epoch, the estimated mean elements and associated uncertainty can be propagated to the subsequent epoch. They can then be compared with the observed mean elements (in the TLE) at the subsequent epoch. If the observed elements are deemed sufficiently unlikely given our propagation and uncertainty, then the epoch is designated as anomalous. More specifically, we compute the negative logarithm of the predictive density of the observation at the subsequent epoch. This figure is taken to be our *anomaly statistic*. After a threshold is chosen, epochs with an anomaly statistic greater than this threshold are designated as anomalous. We expect that the majority of detected anomalies will be the result of manoeuvres, although they could also be the result of changes in the processing of TLEs by the 18<sup>th</sup> Space Defence Squadron, among other reasons (see section 4 for further discussion).

Table 2 contains the specification of all parameters used for filtering.  $\tau_{\text{anom}}$  (the threshold for anomaly detection) was hand-tuned to produce roughly the same rate of anomalies as manoeuvres reported by SpaceX. All other parameters are the same as those used in (Shorten et al., 2023a), apart from the number of particles  $N$ . This was halved for reasons of computational feasibility, given the large number of satellites in the constellation.

This filtering approach was evaluated (Shorten et al., 2023a) on a benchmark dataset containing the TLEs of 15 satellites along with independently-obtained ground-truth manoeuvre timestamps (Shorten et al., 2023b) as well as simulated data. It was demonstrated to be superior to a baseline approach, similar to many previously-proposed approaches for manoeuvre detection from TLE data (Li et al., 2018; Li et al., 2019; Decoto

and Loerch, 2015; Mukundan and Wang, 2021; Zhao et al., 2014).

## 3 RESULTS

### 3.1 Structure of the Starlink Constellation

Much of the following presentation of the results will concern how the timing of manoeuvres is related to the structure of the constellation. As such, we begin with a brief description of this structure.

The Starlink constellation consists of seven orbital shells (see table 3 for a list). The orbits of all satellites in each shell share the same altitude and inclination. The satellites in each shell can be sub-divided into launch groups. These are the 15 to 60 satellites contained in the payload of a single SpaceX rocket launch (Boley et al., 2022; Wikipedia, 2023; McDowell, 2020). All satellites in a given launch group are deployed to the same shell. However, in larger launches, they are split into different sub-groups consisting of around 20 satellites which are deployed to different planes, distinguished by their longitude of the ascending node (Cakaj, 2021; McDowell, 2020).

The orbital shells can themselves be grouped into two constellation generations. The first generation consists of the satellites in the orbits licenced by the FCC on the 28<sup>th</sup> of March 2018. These are the satellites in shells 1, 2, 3, 4, and 6. The second generation consists of the satellites in orbits licenced by the FCC on the 1<sup>st</sup> of December 2022, namely, the satellites in shells 5 and 7 (Federal Communications Commission, 2022; Wikipedia, 2023; McDowell, 2023).

Preliminary analysis indicated that the manoeuvres of the satellites in a given launch group tended to occur close together in time. Much of our analysis, therefore, is performed by grouping the satellites into their launch groups. These groups were determined by using the launch dates included in the list of Starlink satellites obtained from N2YO (N2YO, 2023).

### 3.2 Global Patterns in Manoeuvre Frequency

We first analyse global patterns across the entire constellation of satellites. In order to make this analysis feasible, we investigate the rate of manoeuvres detected within each launch group of satellites. figure 1 plots a heatmap showing the rate of detected manoeuvres (in manoeuvres per satellite per day) within each launch group.

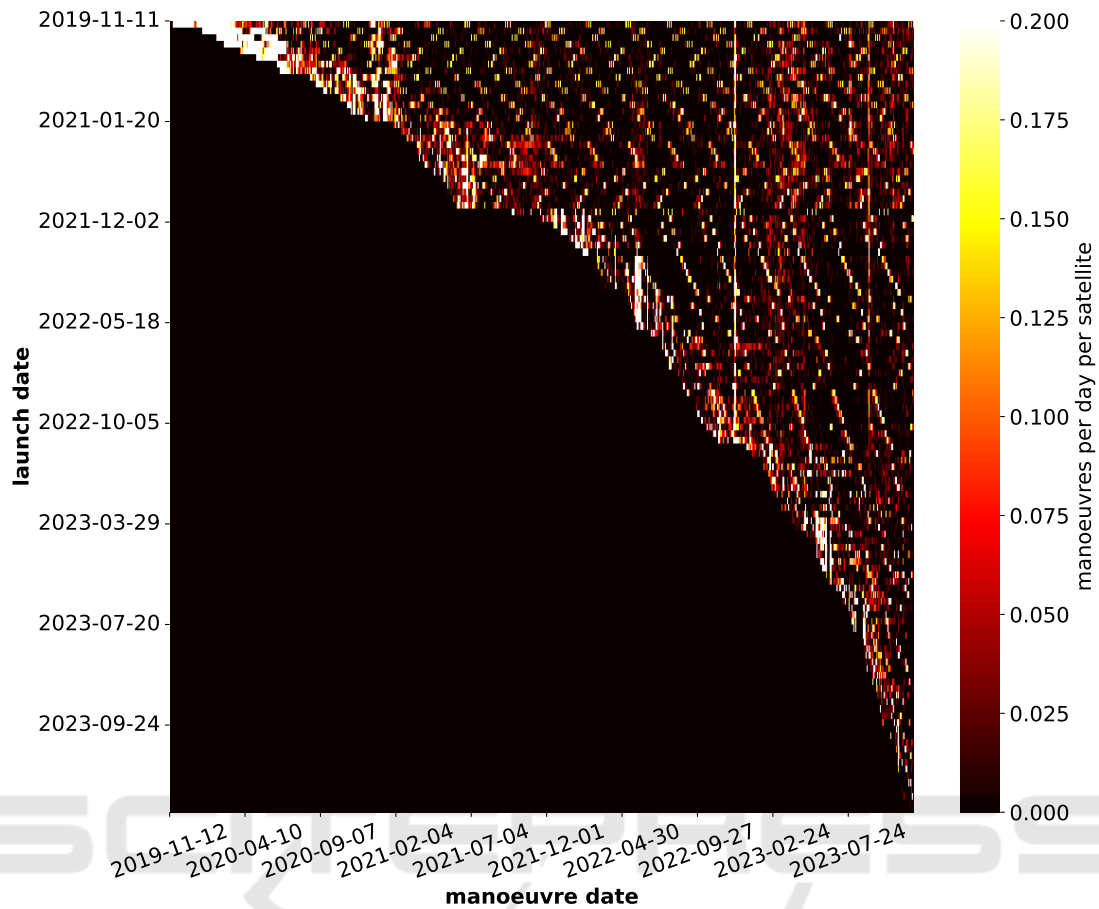


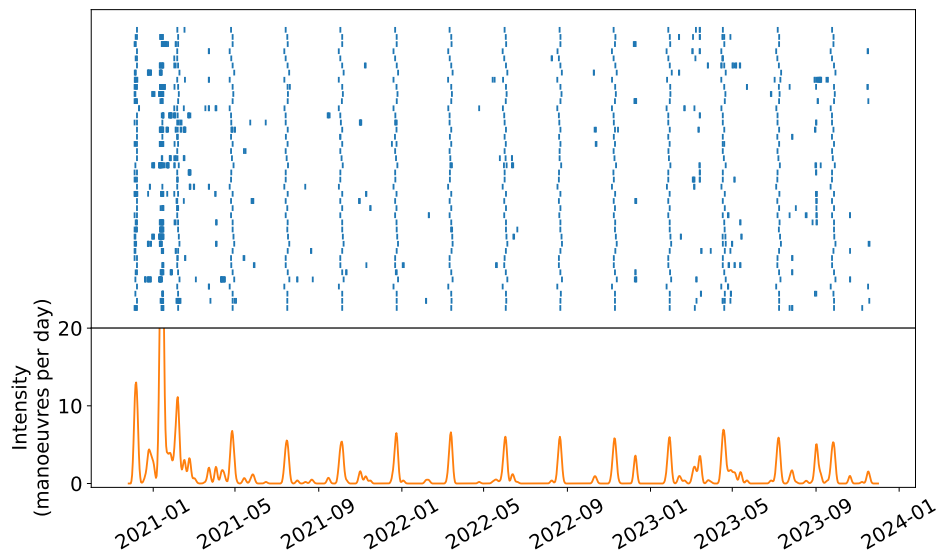
Figure 1: The rate of manoeuvres for the different Starlink satellite launch groups. The rate is estimated using a Gaussian kernel with  $\sigma = 0.5$  days. Note that although the y axis is ordered by the launch dates, these are not equally spaced, and so it does not have a consistent scale. The rate of manoeuvres is particularly high shortly after the launch of each satellite group. There are also pronounced spikes in manoeuvre activity around December 2022 and August 2023.

This plot shows that there is a high incidence of detected manoeuvres near the beginning of each satellite’s time in orbit. After launch, Starlink satellites perform extensive manoeuvring in order to reach their final orbit (Ashurov, 2022). However, in the authors’ experience, TLEs often contain artifacts in the earliest published epochs. It is, therefore, possible that the large number of detected anomalies shortly after launch is partially due to such artifacts.

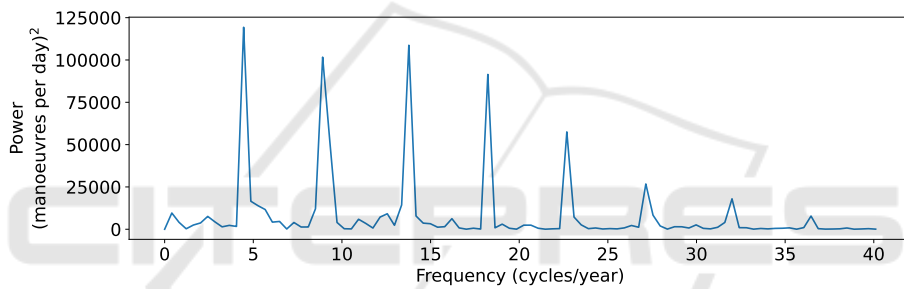
The top right of the plot shows a marked increase in the number of detected manoeuvres for older satellites. This could be being driven by deorbiting manoeuvres or be due to increased incidence of malfunction in these older satellites. There are also two sharp increases in the number of detected manoeuvres that affect most satellites in the constellation. The first, more pronounced, spike occurs on around the 10<sup>th</sup> of December 2022 and the second on around the 2<sup>nd</sup> of September 2023. These spikes could be due to the simultaneous manoeuvring of all or most satellites in

the constellation. However, the authors have encountered instances where the TLE data of multiple unrelated satellites undergo a simultaneous change, likely due to changes in how they are processed by the 18<sup>th</sup> Space Defence Squadron. These spikes could be the result of such an artifact. If they are not the result of an artifact, then it is plausible that the spike on around the 10<sup>th</sup> of December 2022 is the result of an adjustment to the constellation in preparation for the first launch of the 2<sup>nd</sup> generation shell of Starlink satellites, which occurred on the 28<sup>th</sup> of December 2022 (Wikipedia, 2023). See section 3.1 for a description of the two generations of the constellation.

figure 1 also contains multiple lines of higher manoeuvre intensity, at an angle from top left to bottom right. These are likely the result of SpaceX performing sequential station-keeping or maintenance manoeuvres across multiple launch groups. This is further investigate in section 3.5.



(a) Individual manoeuvres and manoeuvre intensity.



(b) Fourier power spectrum of manoeuvre intensity.

Figure 2: A detailed analysis of the manoeuvres of satellite launch group fifteen of shell one. The upper panel of (a) shows the individual inferred manoeuvres for each satellite in the group. Each blue line is the timestamp of a detected manoeuvre and each row contains the manoeuvres of a single satellite in the group. The satellites are ordered by their SATCAT numbers (Kelso, 1998), from top to bottom along the y axis. The lower panel shows an estimate of the intensity of manoeuvre activity, estimated using a Gaussian kernel with a bandwidth of 2 days. (b) shows the Fourier power spectrum of the manoeuvre intensity. The fundamental frequency is at around 4.5 manoeuvres per year, representing an interval of around 80 days between station-keeping manoeuvres.

### 3.3 Regular Station-Keeping Manoeuvring

We now zoom in on a particular launch in order to get a more precise idea of the exact timing of manoeuvres. By selecting a single, representative, launch group we can inspect precise manoeuvre times, as opposed to only examining rates of manoeuvre detections.

The upper panel of figure 2a plots the precise times of detected manoeuvres for each individual satellite in the 15th launch group of shell one. These satellites were launched on the 25<sup>th</sup> of November 2020. After an initial flurry of manoeuvres post launch, regularly-spaced near-synchronous manoeuvring begins — at regular intervals nearly every satel-

lite manoeuvres within a brief one to two day period. Each such burst of manoeuvring is separated by a gap of over 2 months. This regular pattern within the launch group is highly indicative of the detected anomalies being caused by manoeuvres as opposed to artifacts in the TLE data. Moreover, their regularity and synchronicity is indicative of them being station-keeping manoeuvres. The orbits of satellites in low earth orbit, such as the Starlink constellation, degrade over time due to atmospheric drag, solar radiation pressure and the non-spherical nature of the earth (Vallado, 2001). Regular station-keeping manoeuvres are required to maintain the satellites in a roughly constant orbit.

To highlight the periodic nature of these station-keeping manoeuvres, the lower panel of figure 2a

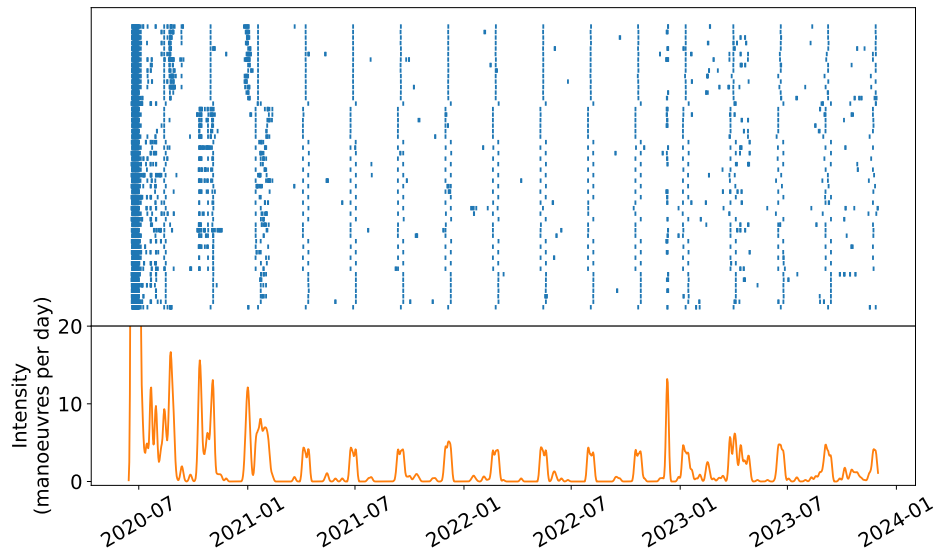


Figure 3: The same plot as in figure 2a, but showing the inferred manoeuvres of launch group eight of shell one. In this older launch group, the stereotyped nature of the station-keeping manoeuvres degrades over time. During the course of 2023, the relative timing of the manoeuvres of the satellites in this group becomes less consistent and some satellites cease manoeuvring during the station-keeping period.

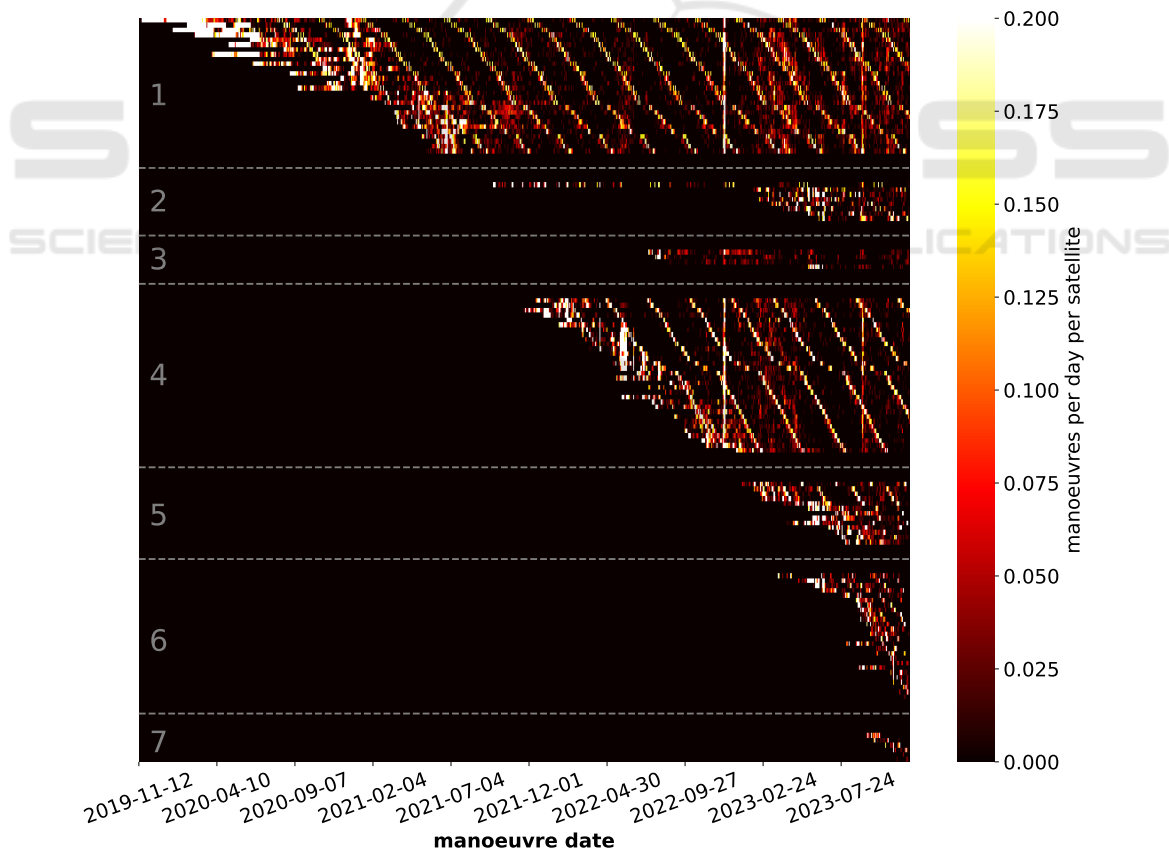


Figure 4: The same plot as figure 1, however, the satellites are reordered along the y axis so that they are grouped into their orbital shells. These shells are separated by the grey dashed lines and their number is given in grey text. The launch groups within each shell have also been reordered so as to emphasize the sequential nature of the regular station-keeping manoeuvres.

Table 3: Various summary statistics and features of the orbital shells. The last column lists the order in which the launch groups of each shell are plotted in figure 4. The numbers in this ordering correspond to the order that the satellites were launched in. The assignment of launch groups to shells is made according to (McDowell, 2023).

Orbit shell number	Number of active satellites	First launch date	Last launch date included	Altitude (km)	Median number of manoeuvres per satellite	Order of launch groups in figure 4
1	1445	11/11/2019	26/5/2021	550	36	1, 3, 2, 4, 7, 6, 9, 5, 12, 8, 13, 10, 15, 14, 11, 18, 16, 19, 23, 17, 20, 21, 22, 25, 24, 28, 26, 27
2	403	14/9/2021	31/5/2023	570	10	1, 4, 5, 6, 7, 8, 9, 10
3	233	11/7/2022	27/4/2023	560	8	1, 2, 3, 5
4	1566	13/11/2021	17/12/2022	540	17	3, 5, 1, 4, 7, 6, 8, 11, 9, 10, 12, 14, 13, 16, 15, 19, 17, 27, 21, 26, 18, 22, 25, 29, 23, 20, 2, 34, 35, 36, 31, 37
5	692	28/12/2022	6/7/2023	530	7	1, 2, 3, 4, 5, 6, 7, 9, 10, 11, 12, 13, 15
6	539	27/2/2023	8/11/2023	559	3	1, 2, 3, 4, 5, 6, 7, 8, 9, 10, 11, 12, 13, 14, 15, 16, 17, 18, 19, 20, 21, 22, 23, 24, 25, 26, 27
7	127	22/8/2023	29/10/2023	525	2	1, 2, 3, 4, 5, 6

plots an estimate of the intensity of manoeuvring in this satellite group. This estimate was performed using a Gaussian kernel with a bandwidth of 2 days. Outside of the increase in manoeuvre activity shortly post launch, the majority of spikes in this intensity correspond to the regularly-spaced bursts in manoeuvres, likely due to station-keeping activity.

figure 2b plots the Fourier power spectrum of the manoeuvre intensity plotted in the lower panel of figure 2a. The fundamental frequency occurs at around 4.5 cycles per year. This corresponds to a period of around 80 days between station-keeping manoeuvres. Both shells one and four had well-defined station-keeping bursts over significant periods of time (see figure 4). All inspected launch groups in these two shells had a similar fundamental frequency and corresponding interval between station-keeping manoeuvres.

Manoeuvres are also detected outside of the station-keeping bursts, likely the result of collision-avoidance manoeuvring (Uriot et al., 2022).

### 3.4 Degradation of Station-Keeping Manoeuvres

We investigate the long-term stability of the station-keeping manoeuvre patterns by plotting the manoeuvre times of the eighth launch group of shell one in figure 3. These satellites were launched on the 13<sup>th</sup> of June 2020 and their behaviour is representative of satellites launched both at a similar time and earlier.

In the earlier parts of these satellites' lifespans, they exhibited a highly-stereotyped pattern of regular manoeuvre bursts. Moreover, the relative ordering of the satellites within each manoeuvre burst was consistent across time.

However, this stereotyped pattern begins to break down, particularly after around February 2023. Each burst of manoeuvres occurs over a broader time interval and the relative time ordering of the satellites is less consistent. Moreover, in the last burst of manoeuvres, no manoeuvres were detected for a number of satellites.

This degradation is likely due to this launch group approaching the end of its lifespan.

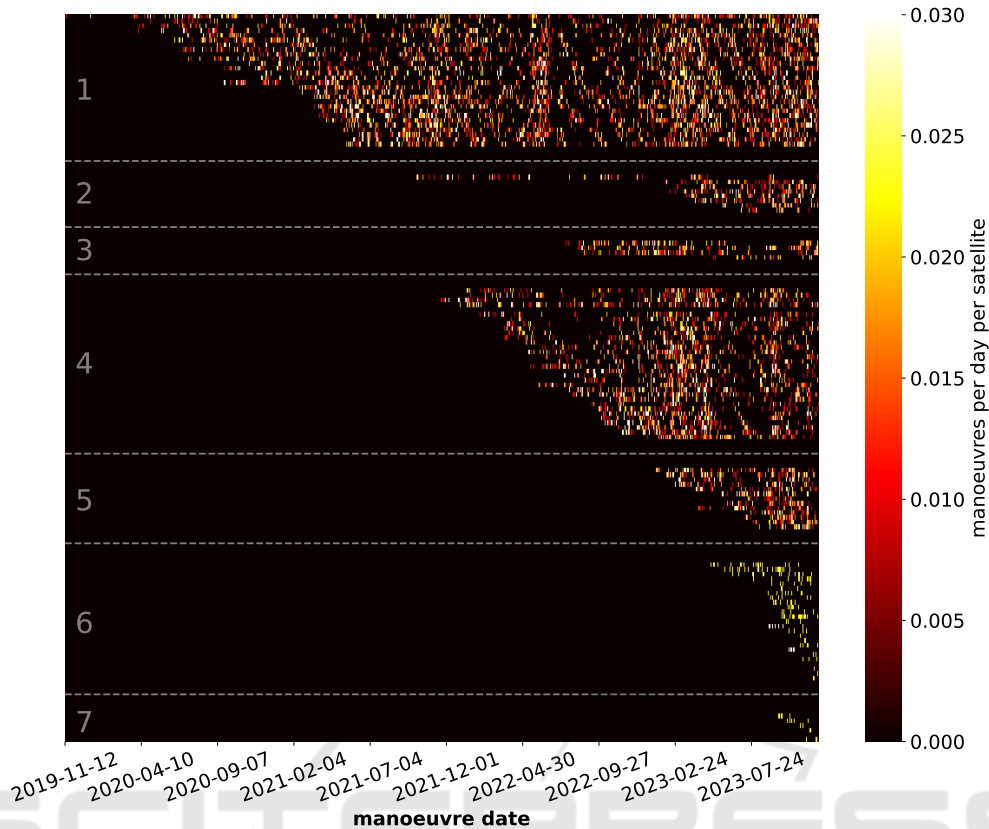


Figure 5: The same plot as figure 1, however, the station keeping and initial positioning manoeuvres have been removed. This was achieved by removing all manoeuvres where the launch group’s manoeuvre intensity was greater than 0.04 manoeuvres per satellite per day. The manoeuvre intensity was subsequently re-estimated after these periods of high intensity were removed. Note that the colours are rescaled from previous figures due to the lower rate of manoeuvres. The majority of remaining manoeuvres should reflect collision-avoidance actions. There are distinct periods of higher or lower incidence of these manoeuvres. For instance, there is a noticeable increase in collision-avoidance manoeuvres in early 2022 for shell one followed by a period of lower activity for the remainder of this year.

### 3.5 Ordering of Station-Keeping Manoeuvres

After establishing that the satellite groups perform periodic group-wide station-keeping manoeuvres, our subsequent analysis concerns the coordination of these station-keeping manoeuvres between the groups. There is a number of ways that SpaceX could coordinate these manoeuvres. For instance, all the satellites in a given shell could manoeuvre simultaneously, or certain supergroups of launch groups could manoeuvre together.

As shown in figure 4, it appears that SpaceX cycles through each launch group within each orbital shell, performing station-keeping manoeuvres in a sequential fashion. This figure plots the manoeuvre intensity of each launch group, similar to figure 1. However, the launch groups have been reordered so that they are grouped into their orbital shells. Moreover,

within shells one and four, the launch groups have been ordered so as to emphasize the sequential nature of the station-keeping manoeuvres, although this was also done so as to maintain the launch order as far as possible. This reordering was not done for the other shells as there were either too few launch groups, or most launch groups had not been active long enough to make such an ordering sensible. Note that, as multiple launch groups within each shell do manoeuvre simultaneously, this ordering is not unique — other orderings of the launch groups will yield a similar pattern to that shown in figure 1.

Within shells one and four, at most three launch groups are undergoing station-keeping manoeuvring at any one point in time. The launch groups are cycled through in an iterative fashion so that all satellites within the shell undergo station-keeping manoeuvres within the roughly 80 day period discussed in section 3.3.

This behaviour makes sense within the context of the management of the constellation. Presumably, manoeuvring might interrupt the transmission of the satellites and SpaceX would therefore want as even a distribution of manoeuvring activity across time as possible.

### 3.6 Trends in Collision Avoidance Manoeuvres

The analysis performed so far has focussed on the constellation's station-keeping activity. However, we know from SpaceX's own filings with the FCC (Goldman, 2023) that the satellites in the Starlink constellation perform a substantial number of collision-avoidance manoeuvres.

We analysed trends in the rate of these manoeuvres over time by removing all station-keeping manoeuvres, before re-analysing the intensity of manoeuvring within each launch group. This was done by first estimating the intensity of manoeuvres within each launch group using a Gaussian kernel with a bandwidth of two days. All manoeuvres that occurred within periods with an estimated intensity above 0.04 manoeuvres per satellite per day were removed. This threshold was chosen through hand-tuning, with the goal being to find the highest threshold for which the pattern of periodic station-keeping manoeuvring disappeared. Note that this process also removes the intense manoeuvre activity that occurs shortly after launch.

After the station-keeping manoeuvres were removed, the manoeuvre rate of each satellite was re-estimated. The resulting manoeuvre rates are plotted in figure 5. This figure reveals that the rate of incidence of collision-avoidance manoeuvres is variable across time. For instance, orbital shell one has a particularly elevated rate of these manoeuvres around April 2022 and February 2023. However, this rate is substantially lower between May 2022 and January 2023. Similar to shell one, shell four has a raised rate of manoeuvres in February 2023, but this is followed by a period of particularly sparse manoeuvring in the middle of 2023.

## 4 DISCUSSION

We applied a recently-developed anomaly detection algorithm for TLE data (Shorten et al., 2023a), to the TLE data of all currently-active Starlink satellites.

A question of primary concern is whether these detected anomalies correspond to the manoeuvres of the Starlink satellites. These anomalies could be

caused by a number of other potential factors, such as artifacts in the TLE data or satellite malfunction. The paper proposing the deployed filtering technique for anomaly detection (Shorten et al., 2023a) performed a thorough evaluation of its accuracy. This was performed on a benchmark dataset (Shorten et al., 2023b) which contained the TLEs of 15 satellites and associated independently-obtained ground-truth manoeuvre timestamps. This dataset contained a mixture of satellites in geosynchronous and low-earth orbits, which is where the Starlink constellation is situated. It was demonstrated that this approach was able to achieve fairly high performance on most satellites, achieving F1 scores over 0.8 in many cases. However, these scores are not perfect. Moreover, no validation of this approach has been performed on Starlink satellites, which make use of electric propulsion (Holste et al., 2020) compared with the chemical propulsion of the satellites in the benchmark dataset. It is therefore almost certain that some of the anomalies detected in the Starlink TLE data are false positives. It is also highly likely that some manoeuvres went undetected.

That being said, there are features of the patterns of detected anomalies which should increase our confidence in the results. As discussed in section 3.3, there are regular bursts of manoeuvres where an anomaly is detected for all satellites in one launch group within a narrow period (around a day). Moreover, as shown in figure 4, different satellite groups rarely exhibit such bursts of anomalies simultaneously. This behaviour is easy to explain if the detected anomalies are station-keeping manoeuvres being performed across all satellites on the same or similar orbital plane. However, it is difficult to see why artifacts in TLEs would line up so precisely based on the satellite's launch date or orbital plane. The consistent relative timing of the manoeuvres of each satellite in a launch group during the station-keeping manoeuvres, as discussed in section 3.3, is similarly better explained by patterns in how SpaceX is choosing to manoeuvre its satellites than by patterns in the distribution of artifacts in TLE data.

The Starlink constellation exhibits a rich pattern of detected manoeuvres across time and the different satellite launch groups. figure 1 provides a global summary of the detected manoeuvres by plotting a heatmap of the rate of detected manoeuvres within each satellite group. The rate of manoeuvres was generally higher shortly after launch and in the latter parts of older satellites' lifespans. There are also some noticeable spikes in manoeuvring activity, such as around the 10<sup>th</sup> of December 2022.

More detailed analysis of the precise manoeuvre times of individual satellites reveals further structure.

figure 2 plots the precise manoeuvre times for all satellites in a representative launch group. The group undergoes regularly-spaced bursts in manoeuvring activity, where all satellites in the group manoeuvre near-simultaneously. Moreover, the relative ordering of the manoeuvres within the bursts remains consistent over time. The frequency of these bursts in both the representative launch group as well as in other launch groups studied was around 4.5 bursts per year, giving a corresponding period of around 80 days between bursts. These bursts are likely the result of regular station-keeping manoeuvres being performed by SpaceX. Anomalies unique to individual satellites are also detected outside of these bursts. It is likely that a significant proportion of such anomalies are the result of collision-avoidance manoeuvres by SpaceX.

The regularity of the station-keeping manoeuvres was shown to break down over time in certain satellites. figure 3 plots the precise manoeuvre times of an early launch group. In the earlier parts of their lifespan, the satellites exhibit a highly stereotyped pattern of manoeuvres, with the relative ordering of the satellites within each burst remaining highly consistent. This consistency breaks down close to the present day. Moreover, some satellites no longer manoeuvre in the bursts.

Section 3.5 studied the relationship in the timing of the station-keeping manoeuvre bursts between the launch groups of each shell. The launch groups rarely performed their station-keeping manoeuvres simultaneously. Instead, it appears that SpaceX moves through the different launch groups in an iterative fashion so as to minimize the number of satellites manoeuvring simultaneously.

Finally, 3.6 studied the incidence of collision avoidance manoeuvres in the constellation by removing the station-keeping manoeuvres from the analysis and examining the remaining manoeuvres. It was found that the different shells of the constellation go through distinct periods of increased or decreased collision-avoidance manoeuvring activity.

## 5 CONCLUSION

Due to the anticipated rapid increase in their size, large satellite constellations such as Starlink will increase the difficulty of space traffic management. However, little is currently known about how SpaceX manages this constellation and, in particular, how it manoeuvres the satellites within it. This work addressed this lack of insight by applying a recently-developed anomaly detection algorithm to the TLE data of all satellites currently active in the Starlink

constellation. It was found that satellites undergo an initial period of rapid manoeuvring before settling into a state dominated by regular bursts in the manoeuvring of all satellites within a particular launch group to perform station keeping. These bursts are interspersed with isolated collision-avoidance manoeuvres. This pattern of regular bursting degrades over time in the earliest launches.

## ACKNOWLEDGEMENT

We thank Will Heyne of BAE Systems for helpful insights throughout the course of this research. This work has been supported by the SmartSat CRC, whose activities are funded by the Australian Government's CRC Program.

## REFERENCES

- Ashurov, A. E. (2022). An effective method for detecting satellite orbital maneuvers and its application to LEO satellites. *Advances in Aircraft and Spacecraft Science*, 9(4):279.
- Boley, A. C. and Byers, M. (2021). Satellite mega-constellations create risks in low earth orbit, the atmosphere and on earth. *Scientific Reports*, 11(1):10642.
- Boley, A. C., Wright, E., Lawler, S., Hickson, P., and Balam, D. (2022). Plaskett 1.8 m observations of Starlink satellites. *The Astronomical Journal*, 163(5):199.
- Cakaj, S. (2021). The parameters comparison of the Starlink LEO satellites constellation for different orbital shells. *Frontiers in Communications and Networks*, 2:643095.
- Decoto, J. and Loerch, P. (2015). Technique for GEO RSO station keeping characterization and maneuver detection. In *Advanced Maui Optical and Space Surveillance Technologies Conference*, page 42.
- Federal Communications Commission (2022). FCC 22-91.
- Goldman, D. (2023). SpaceX constellation status report, December 1, 2022 to May 31, 2023. Technical report, Space Exploration Technologies Corp.
- Holste, K., Dietz, P., Scharmann, S., Keil, K., Henning, T., Zschätzsch, D., Reitemeyer, M., Nauschütt, B., Kiefer, F., Kunze, F., et al. (2020). Ion thrusters for electric propulsion: Scientific issues developing a niche technology into a game changer. *Review of Scientific Instruments*, 91(6).
- Kelso, T. (1998). Frequently asked questions: Two-line element set format. [celestrak.org/columns/v04n03/](http://celestrak.org/columns/v04n03/). Accessed: 2022-10-26.
- Lal, B., Balakrishnan, A., Caldwell, B. M., Buenconsejo, R. S., and Carioscia, S. A. (2018). Global trends in Space Situational Awareness (SSA) and Space Traffic Management (STM). *Science and Technology Policy Institute*, 10.

- Li, T., Li, K., and Chen, L. (2018). New manoeuvre detection method based on historical orbital data for low earth orbit satellites. *Advances in Space Research*, 62(3):554–567.
- Li, T., Li, K., and Chen, L. (2019). Maneuver detection method based on probability distribution fitting of the prediction error. *Journal of Spacecraft and Rockets*, 56(4):1114–1120.
- McDowell, J. (2020). The low earth orbit satellite population and impacts of the SpaceX Starlink constellation. *The Astrophysical Journal Letters*, 892(2):L36.
- McDowell, J. (2023). Jonathan’s space pages - Starlink statistics. [planet4589.org/space/con/star/stats.html](http://planet4589.org/space/con/star/stats.html). Accessed: 2023-12-10.
- Michel, F., Trevisan, M., Giordano, D., and Bonaventure, O. (2022). A first look at starlink performance. In *Proceedings of the 22nd ACM Internet Measurement Conference*, pages 130–136.
- Mukundan, A. and Wang, H.-C. (2021). Simplified approach to detect satellite maneuvers using TLE data and simplified perturbation model utilizing orbital element variation. *Applied Sciences*, 11(21):10181.
- N2YO (2023). Starlink satellites. [www.n2yo.com/satellites/?c=52](http://www.n2yo.com/satellites/?c=52). Accessed: 2023-11-30.
- Pelton, J. N. (2015). *New solutions for the space debris problem*. Springer.
- Shorten, D. P., Maclean, J., Humphries, M., Yang, Y., and Roughan, M. (2023a). Optimal proposal particle filters for detecting anomalies and manoeuvres from two line element data. *arXiv preprint arXiv:2312.02460*.
- Shorten, D. P., Yang, Y., Maclean, J., and Roughan, M. (2023b). Wide-scale monitoring of satellite lifetimes: Pitfalls and a benchmark dataset. *Journal of Spacecraft and Rockets*, pages 1–5.
- Snyder, C. (2011). Particle filters, the “optimal” proposal and high-dimensional systems. *ECMWF Seminar on Data assimilation for atmosphere and ocean*, page 10.
- Space-Track (2023). SPACE-TRACK.ORG. [space-track.org](http://space-track.org). Accessed: 2023-12-05.
- SpaceX (2023). Launches. [www.spacex.com/launches/](http://www.spacex.com/launches/). Accessed: 2023-12-05.
- Union of Concerned Scientists (2023a). How many satellites are in space? the spike in numbers continues. [blog.ucsusa.org/syoung/how-many-satellites-are-in-space-the-spike-in-numbers-continues/](https://blog.ucsusa.org/syoung/how-many-satellites-are-in-space-the-spike-in-numbers-continues/). Accessed: 2023-12-04.
- Union of Concerned Scientists (2023b). UCS satellite database. [www.ucsusa.org/resources/satellite-database](http://www.ucsusa.org/resources/satellite-database). Accessed: 2023-12-04.
- Uriot, T., Izzo, D., Simões, L. F., Abay, R., Einecke, N., Rebhan, S., Martínez-Heras, J., Letizia, F., Siminski, J., and Merz, K. (2022). Spacecraft collision avoidance challenge: Design and results of a machine learning competition. *Astrodynamics*, 6(2):121–140.
- Vallado, D., Crawford, P., Hujsak, R., and Kelso, T. (2006). Revisiting spacetrack report #3. In *AIAA/AAS Astrodynamics Specialist Conference and Exhibit*, page 6753.
- Vallado, D. A. (2001). *Fundamentals of astrodynamics and applications*, volume 12. Springer Science & Business Media.
- Vallado, D. A. and Cefola, P. J. (2012). Two-line element sets - practice and use. In *63rd International Astronautical Congress, Naples, Italy*, pages 1–14.
- Venkatesan, A., Lowenthal, J., Prem, P., and Vidaurri, M. (2020). The impact of satellite constellations on space as an ancestral global commons. *Nature Astronomy*, 4(11):1043–1048.
- Wikipedia (2023). List of Starlink and Starshield Launches. [en.wikipedia.org/wiki/List\\_of\\_Starlink\\_and\\_Starshield\\_launches](https://en.wikipedia.org/wiki/List_of_Starlink_and_Starshield_launches). Accessed: 2023-12-10.
- Zhao, Y., Zhang, K., Bennett, J., Sang, J., and Wu, S. (2014). A method for improving two-line element outlier detection based on a consistency check. In *Proceedings of the Advanced Maui Optical and Space Surveillance (AMOS) Technologies Conference, Maui, Hawaii*.